Journal of Membrane Science 595 (2020) 117585

Contents lists available at ScienceDirect

Journal of Membrane Science

journal homepage: http://www.elsevier.com/locate/memsci

Sulfonated polyethersulfone based cation exchange membranes for reverse electrodialysis under high salinity gradients

Ahmet H. Avci [a], Timon Rijnaarts [b], Enrica Fontananova [c], Gianluca Di Profio [c], Ivo F. V. Vankelecom [d], Wiebe M. De Vos [b], Efrem Curcio [a,c,*]

[a] Department of Environmental and Chemical Engineering, University of Calabria, DIATIC-UNICAL, Via P. Bucci CUBO 45A, 87036, Rende, CS, Italy
[b] Membrane Science & Technology, University of Twente, P.O. Box 217, 7500 AE, Enschede, the Netherlands
[c] Institute on Membrane Technology, National Research Council of Italy ITM-CNR, Via P. Bucci CUBO 17C, 87036, Rende, CS, Italy
[d] Centre for Surface Chemistry and Catalysis, Faculty of Bio-Science Engineering, KU Leuven, Celestijnenlaan 200F, PO Box 2461, 3001, Leuven, Belgium

ARTICLE INFO

Keywords:
Reverse electrodialysis
Salinity gradient power
Cation exchange membrane
Sulfonated polyethersulfone
Electrochemical impedance spectroscopy

ABSTRACT

Salinity Gradient Power - Reverse Electrodialysis (SGP-RED) is a promising membrane-based technology to harvest the energy of mixing from solutions of different ionic concentration. Unfortunately, currently available commercial ion exchange membranes – being not specifically designed for RED – are far from satisfying the requirements of this operation, especially when operated with hyper-concentrated brines. In this work, novel sulfonated polyethersulfone (sPES) cation exchange membranes (CEM) were prepared by phase inversion method and tested under high salinity gradients. Use of 5 M NaCl electrolyte for immersion precipitation coagulation bath facilitated the self-standing membrane formation as a result of the electrostatic interaction between the fixed charged groups and electrolyte solution. Microscopy results revealed that dense or asymmetric membranes with non-connected pores were formed by solvent evaporation or immersion precipitation, respectively. The membranes were characterized for ion exchange capacity, water uptake, charge density and thickness, and further studied by electrochemical impedance spectroscopy. The obtained properties of the newly developed membranes were subsequently compared to those of commercial CMX (Neosepta, Japan) and Fuji-CEM-Type 1 (Fujifilm, The Netherlands) membranes. The asymmetric membranes resulted in a very low resistance especially for high ionic gradients but relatively low permselectivity, while dense membranes still had a low resistance compared to commercial membranes and exhibited high permselectivity. Interestingly, in terms of power density, lab-made membranes outperformed the commercial benchmarks when tested for RED applications with brackish water (0.1 M NaCl)/hypersaline brine (4 M NaCl) feeds; power density of CMX and Fuji-CEM-Type 1 were 3.23 and 3.77 W/m^2, respectively, while power density of asymmetric and dense sPES membranes were 3.64 and 3.92 W/m^2, respectively.

1. Introduction

Salinity Gradient Power (SGP), the energy that can be harvested from the mixing of solution of different ionic strength, has regained worldwide attention in the past decade after having been introduced as early as 1954 by Pattle et al. [1]. With an estimated global potential energy between 0.23 and 3.13 TW, SGP is a promising approach to alternative renewable energy to help the transition towards a low-carbon economy [2]. River mouths, where two solutions with different salinity meet, are considered the largest natural SGP sources [3]. Moreover, saline groundwater [4], saltworks [5], salt lakes, brines of natural and oil gas fields [6], brines from desalination units (e.g., reverse osmosis [7,8] and membrane distillation [9–11]) are increasing in interest as more energy intensive SGP effluents. A key benefit compared to renewable energy sources such as solar and wind energy is that salinity gradients are much less susceptible to fluctuations, ensuring a more stable source of power.

Among different approaches, pressure retarded osmosis (PRO) and reverse electrodialysis (RED) are the most promising membrane-based technologies for SGP energy generation [12–14]. Main advantages of PRO against RED are the possibility to utilize higher power density and

* Corresponding author. Department of Environmental and Chemical Engineering, University of Calabria, DIATIC-UNICAL, Via P. Bucci CUBO 45A, 87036, Rende, CS, Italy.
E-mail address: e.curcio@unical.it (E. Curcio).

https://doi.org/10.1016/j.memsci.2019.117585
Received 15 May 2019; Received in revised form 23 September 2019; Accepted 18 October 2019
Available online 22 October 2019

efficiency especially when high salinity solutions are fed and relatively lower cost of the membranes [15,16], whereas RED is advantageous for being less sensitive to fouling [17] and allowing a direct conversion of electricity from salinity gradients [15]. As illustrated in Fig. 1, a typical RED unit consists of alternately arranged anion exchange membranes (AEM) and cation exchange membranes (CEM) which are separated by spacers to create adjacent channels. By pumping diluted/concentrated saline solutions into the channels, an electrochemical potential gradient is generated, driving the ions from high to low concentration. Due to the charged nature of the membranes, ions can only diffuse through the oppositely charged membranes (i.e. positive ions can diffuse through CEM, while negative ions diffuse through AEM). By utilizing electrodes at both ends of the RED stack, the selective ionic flux across the membranes is converted into an electronic flux by redox reactions [11].

Ion exchange membranes (IEM) are the most critical performance determining elements in RED. In general, IEMs are utilized in the various electromembrane processes were designed to satisfy the requirements of specific applications. For example, permselectivity is essential for purification applications, i.e. electrodialysis (ED), whilst chemical and thermal stability of membranes is more important for the chlor-alkali process [18]. The majority of the membranes investigated for RED operation are commercial membranes specifically developed for ED due to similarity of both processes [19,20]. However, the needs for RED differ from those for ED. In order to maintain permselectivity in ED, membranes have a high charge density and are mostly reinforced with another stable material against swelling, resulting in relatively thick membranes. Moreover, ED membranes were designed for challenging conditions, such as high current density and extreme pH conditions [21,22]. On the other hand, RED conditions are rather mild: process solutions are generally close to neutral pH, and just a low hydrostatic pressure is applied to flow solutions across the inlet and outlet of compartments.

Most of the commercial ion exchange membranes are produced as dense homogeneous membranes by functionalized polymeric materials. These membranes have a permselectivity higher than 90%, an areal resistance between 1 and 5 $\Omega \cdot cm^2$, an IEC between 1.1 and 2.5 $meq \cdot g^{-1}$, a water uptake up to 30% and a thickness between 30 and 200 μm [18,23,24]. All these properties are interrelated and most often counter-acting against each other [25]. For example, a high IEC capacity means a high permselectivity and low resistance up to a certain degree. Beyond this degree, increasing IEC leads high swelling which reduces the number of functional group per volume, leading IEM to inefficient Donnan exclusion so the permselectivity and resistance decrease [26].

So far, the biggest obstacle hampering commercialization of RED is the absence of tailored IEMs for high power density generation, occurring when operated under high salinity gradient: a feasible RED membrane must have a high permselectivity, a low resistance, sufficient mechanical and chemical stability and a low price. Post et al. (2009) studied the requirements of RED membranes; for a cost-effective operation, the membrane should have a selectivity higher than 95%, a resistance lower than 3 $\Omega \cdot cm^2$, mechanical stability that is sufficient to construct the stack for a lifetime of at least 5 years and a maximum price of 2 €/m^2 [27].

Regarding their structure and preparation procedure, ion exchange membranes can be classified into two main categories [28]: heterogeneous membranes having high selectivity, mechanical stability, low price but high ionic resistance (>10 $\Omega \cdot cm^2$), and homogeneous membranes having good mechanical and electrochemical properties, but being rather expensive (>100 €/m^2). Among these limiting parameters, the price of the membrane is the most challenging for the near future [22,27,29,30].

Several studies have been made to prepare IEMs specifically for RED. Tailor-made IEMs were prepared by using sulfonated polyetheretherketone (SPEEK) and polyepichlorohydrin (PECH), and then tested in artificial seawater and river water conditions in a lab-scale RED stack: a maximum power density of 1.28 W/m^2 was obtained for the stack operated with SPEEK/PECH membranes couple, while the one obtained with FKD/FAD commercial membranes was 1.19 $W \cdot m^{-2}$ [26].

Novel composite membranes were prepared by embedding Fe_2SO_4–SO_4^{2-} charged inorganic particles into PPO. The membrane properties were characterized for different loading ratio's and finally tested in RED stack: the highest gross power density obtained was 1.30 $W \cdot m^{-2}$ for 0.7 wt% loading [31].

Recently, AEMs and CEMs were prepared by a pore filling technique. Physicochemical and electrochemical characterizations revealed that the membranes had comparable permselectivity and mechanical stability, but a four times lower areal resistance than commercial membranes (i.e. FKS and FAS from FumaTech GmbH, Germany, CMX and AMX from Takuyama Com, Japan; CMV and AMV from Asahi Glass Co. Ltd, Japan). Moreover, a 2.4 $W \cdot m^{-2}$ gross power density was reported using KIER pore-filling membranes: this value was 25% higher compared to the best performing commercial membrane pair (AMX/CMX) [32].

In this work, we developed novel CEMs from sulfonated polyethersulfone (sPES) specifically optimized for RED applications under hyper-concentrated saline solutions. To our knowledge, for the first time sPES lab-made CEMs were prepared and characterized for their RED potential, with specific focus on operations at high salinity gradients in order to exploit the electrochemical potential of brines. Traditionally, the morphology of ion exchange membranes is dense to allow efficient Donnan exclusion [33]. According to our conceptual strategy, the design of ion exchange membranes with more open structure that maintains

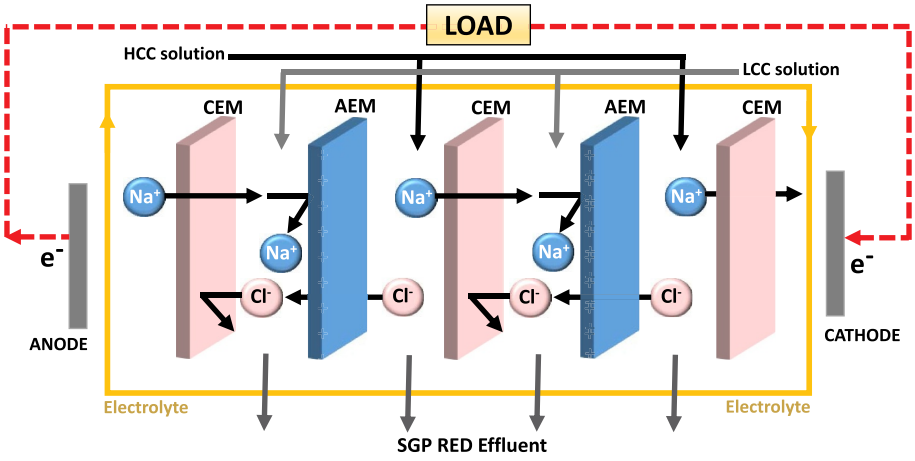

Fig. 1. Schematic representation of a RED unit ([23]).

co-ion exclusion is expected to enhance the ion conductivity due to a larger interstitial volume. As a consequence, the performance of RED is projected to increase especially when operated with highly concentrated saline feeds.

As a further advantage, the adopted membrane manufacturing approach is potentially scalable at industrial level: investigated preparation methods include either solvent evaporation, leading to dense membranes, or solvent exchange by immersion precipitation [34], leading a more open membrane with non-connected cell-like pores. Electrochemical characterization of commercial CMX and Fuji CEM Type 1 used as a target, along with lab-made sPES membranes, was carried out by permselectivity tests and electrochemical impedance spectroscopy for high salinity gradients. Moreover, single cell RED experiments for four CEMs were performed at 0.1/4.0 M NaCl and 25 °C.

2. Experimental

2.1. Materials

Sulfonated polyethersulfone (sPES) with 1.19 meq·g^{-1} ion exchange capacity (IEC) and 119,000 g·mol^{-1} molecular weight was provided by Konishi Chemical Ind. Co. Ltd., Japan.

Fuji CEM Type 1 (Fuji-CEM) was kindly supplied from Fujifilm, The Netherlands. Neosepta CMX cation exchange membrane was purchased from Astom Corp. Ltd., Japan.

1-Methyl-2-pyrrolidinone (NMP, 99%) was supplied from Sigma-Aldrich, The Netherlands. Technical grade NaCl was purchased from VWR, Italy. Hydrochloric acid 37% and sodium hydroxide 1 M were purchased from Carlo Erba, Italy and Fluka Analytical, Italy, respectively.

2.2. Membrane preparation

For the solvent evaporation method, NMP-based solutions of 20 wt% sPES were prepared. Polymer solutions were cast on a glass plate using a knife with a 500 μm opening. After casting, films were dried under N_2 atmosphere at 70 °C for 2 days; finally, the membranes were easily peeled off in demi-water. Samples were kept in 0.5 M NaCl solution until further use.

For membranes prepared by immersion precipitation, NMP-based solutions were prepared with 30 wt% sPES. The polymer solution was cast on a glass plate using a casting knife with a 250 μm opening. After that, the polymer film was immersed into a 5 M NaCl solution and a white-colored membrane was formed in less than 30 s. The final product was kept in a 0.5 M NaCl solution before further characterization.

Physical appearance of commercial and lab-made cation exchange membranes are shown in Fig. 2.

2.3. Membrane characterization

2.3.1. Ion exchange capacity

The ion exchange capacity (IEC) of cation exchange membranes was measured by acid-base titration method. Membrane samples were immersed into excess 1 M HCl solution for 24 h to saturate all the fixed charged groups with H^+; then the samples were washed with demi-water until the surface water was completely removed. Following this, the samples were immersed into 40 ml of 2 M NaCl solution to exchange H^+ with Na^+ and to release H^+ into solution. This step was repeated 3 times for a complete exchange. Finally, the immersed solutions were collected into a beaker and titrated with 0.01 M NaOH. The titration was continued until the pH of the collected solution reached the pH of the initial 2 M NaCl solution [35]. The pH values were monitored with a pH meter (WTW Inolab Terminal Level 3, Germany). The IEC (meq·g dry membrane^{-1}) was calculated by using the following equation:

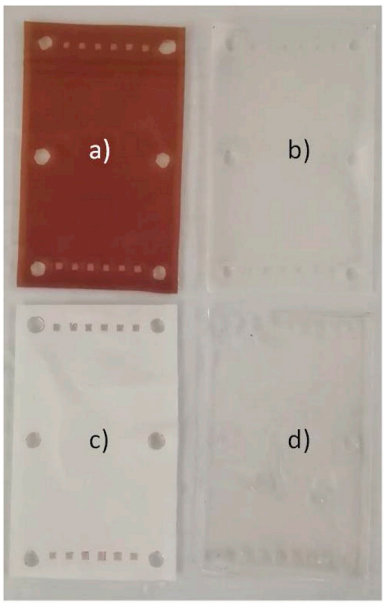

Fig. 2. Physical appearance of a) CMX, b) Fuji-CEM-Type1, sPES-P and b) sPES-D.

$$IEC = \frac{V_{NaOH} \cdot M_{NaOH}}{m_{dry}} \quad (1)$$

in which V_{NaOH} is volume of NaOH titrant (l), M_{NaOH} is molarity of NaOH titrant (mol·l^{-1}) and m_{dry} is the dry weight of the sample (g) after washed with water and left in an oven at 70 °C for overnight. The reported IEC values are the average of at least 3 repetition.

2.3.2. Water uptake and fixed charge density

The water uptake (wu) of the CEMs was calculated by gravimetric method, according to the following formula:

$$wu = \frac{m_{swelled} - m_{dry}}{m_{dry}} \cdot 100 \quad (2)$$

where $m_{swelled}$ is the swelled membrane weight after immersion in 0.5 M NaCl, and m_{dry} is the dry weight of the membrane left in oven at 70 °C overnight. The reported water uptake values are the average of at least 3 repetition.

By definition, fixed charge density (c_{fix}) means mmol of fixed charge groups in a unit volume of water and can be determined by using IEC and water uptake as below indicated:

$$c_{fix} = \frac{IEC \cdot d}{wu} \cdot 100 \quad (3)$$

where d is the density of water at 25 °C.

2.3.3. Permselectivity

A two-compartment cell (Fig. 3) was operated at 25 °C to determine the membrane potential. Before measurements, membranes were conditioned overnight in the low concentrated solution (i.e. the conditioning solution was 0.1 M NaCl in case the measurement was carried out for 0.1/0.5 M NaCl). Then, membrane was sandwiched between compartments and the membrane potential measured in 0.1/0.5, 0.1/4.0 and 0.5/4.0 M NaCl solutions. The solutions were recirculated through the compartments by two gear pumps at a flow rate of 460 ml·min^{-1} and 25 °C. Potential difference over the electrodes was recorded until constant values were obtained. Finally, permselectivity (α) was calculated from the ratio between the measured membrane potential (V) and the theoretical membrane potential (V) which

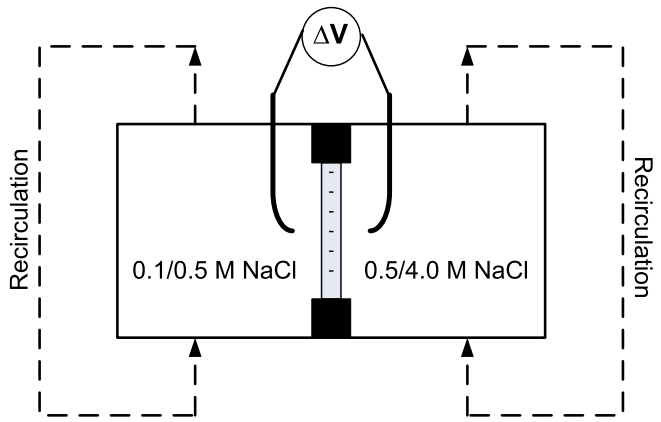

Fig. 3. Two compartment permselectivity characterization setup.

represents 100% permselectivity:

$$\alpha(\%) = \frac{\Delta V_{measured}}{\Delta V_{theoretical}} 100\% \quad (4)$$

$\Delta V_{theoretical}$ is calculated by the Nernst equation:

$$\Delta V_{theoretical} = \frac{RT}{zF} \ln\left(\frac{C_2\gamma_2}{C_1\gamma_1}\right) \quad (5)$$

in which R is the gas constant ($J \cdot mol^{-1}K^{-1}$), T the temperature (K), z the electrochemical valence (−), F the Faraday constant (96485 $s \cdot A \cdot mol^{-1}$), C_1 and C_2 the concentrations of the two solutions ($mol \cdot l^{-1}$), and γ_1 and γ_2 the activity coefficients of the two solutions. Table 1 presents the theoretical membrane potentials and the activity coefficients for different solution pairs calculated by eq. (5). The reported permselectivity values are the average of 2 repetition.

2.3.4. Resistance – electrochemical impedance spectroscopy

To measure ionic resistance, electrochemical impedance spectroscopy (EIS) experiments were conducted with a potentiostat/galvanostat assisted with a frequency response analyzer (Metrohm Autolab PGSTAT302 N) as described elsewhere [35]. A home-made cell having two compartment and four electrodes allowing 3.14 cm^2 active membrane area was designed for ionic resistance characterization (Fig. 4). The planar electrodes (working and counter electrode) were made of Ag while reference electrodes (sense and reference electrode, immersed in Haber-Lugging capillaries filled with 3 M KCl) were Ag/AgCl from Gamry Instruments; the Haber–Luggin capillaries were filled with KCl 3 M. The cell was operated inside of a Faraday cage to avoid the external disturbance.

Each cell compartment was fed with a separate gear pump that recirculates 1 L solution at a 460 ml/min flow rate and 25 ± 2 °C temperature. The solution concentration in both compartment were same; 0.1, 0.5, 1.0, 2.0 or 4.0 M NaCl solution. The cation exchange membranes were conditioned in the test solution for at least 16 h.

Alternate current in the frequency range of 1000–0.01 Hz with a 10 mV signal amplitude was generated through the planar electrodes and the response of the membrane-interface system was recorded by measuring potential drop over the membrane. Fig. 5 shows the equivalent circuit model fitting the collected data. The equivalent circuit includes solution plus membrane (m + s) resistance represented by a resistor, the electrical double layer (edl) represented by a parallel resistor and capacitor, and the diffusion boundary layer (dbl) resistance represented by a resistor and a constant phase element. Before and after each experiment, a blank experiment (without the membrane) was repeated under same conditions to measure solution resistance. Then, the areal membrane resistance was calculated by subtracting the average solution resistance from R_{m+s} and multiplying it by the active membrane area. Each experiment was repeated at least two times and the average data was reported.

Table 1
Activity coefficient and theoretical membrane potential of solution pairs.

Concentration (M NaCl)	Activity coefficient [36] (−)	Test solution pair (M NaCl/M NaCl)	Theoretical ΔV (mV)
0.1	0.778	**0.1/0.5**	37.9
0.5	0.681	**0.1/4.0**	96.0
4.0	0.815	**0.5/4.0**	58.0

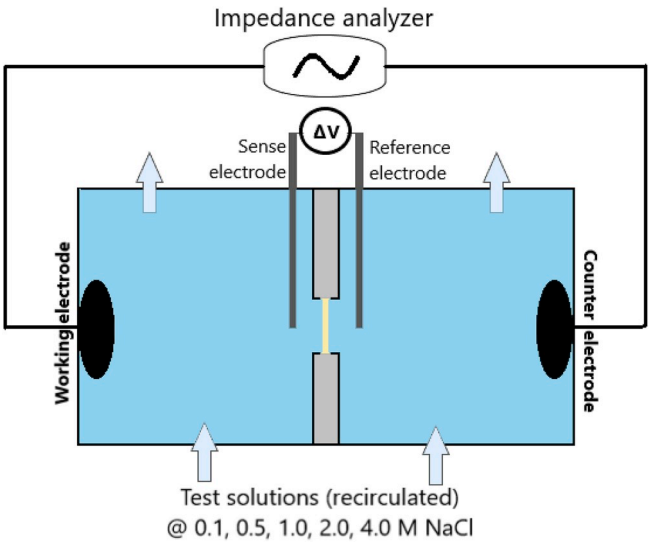

Fig. 4. EIS characterization cell.

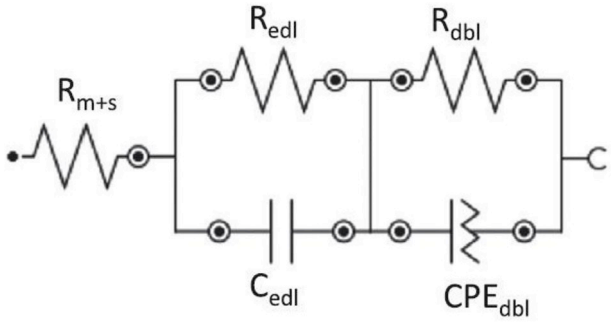

Fig. 5. Equivalent circuit used to fit EIS spectra.

2.3.5. Morphology

The cross-sections of membranes were observed by EVO MA10 Zeiss scanning electron microscopy. Top-layer cross-section images at 20000 magnification were captured for sPES membranes.

2.3.6. Reverse electrodialysis stack

The lab-scale electrodialysis cell (PCCell 200) provided by PCCell GmbH (Germany) was used in reverse electrodialysis mode to characterize electrochemical performance of the stack equipped with aforementioned CEMs paired with AMX (Neosepta, Japan). CEMs were cut into 26.2 × 12.5 cm^2 pieces to fit 500 μm thick spacers which allows 207 cm^2 active area. The electrode compartments include anode and cathode made of inert Pt/Ir-coated Titanium mesh. The electrode compartments were separated from central compartments by CMX membranes.

Feed solutions were prepared by dissolving appropriate amount of

NaCl in deionized water (PURELAB, Elga LabWaters, 0.055 mS·cm^{-1}). The composition of aqueous electrolyte solution was: 0.3 M potassium ferricyanide, 0.3 M potassium ferrocyanide and 2.5 M sodium chloride (Sigma-Aldrich S.r.l., Italy).

The performance of the SGP-RE unit was investigated at 25 °C and linear flow velocity of concentrated (4 M NaCl) and diluted (0.1 M NaCl) compartments were 3 cm s^{-1}. Flowrate of electrolyte solution was fixed to 15 L·h^{-1}. Solutions were fed by Masterflex L/S digital peristaltic pumps (Cole-Palmer, US) and conditioned to desired temperature by a refrigerated/heated circulating bath (PolyScience, US) before entering the stack.

A high dissipation five-decade resistance box (CROPICO, Bracken Hill, US) was used to load the stack. DC voltage drop across the stack was measured by a 3½ digital multimeter with accuracy of 70.5% in the range of 200 mV to 200 V (Velleman, DVM760, Belgium), and the current flowing across the load resistors was measured by 6½ digit multimeter (Agilent, 34422A, Italy).

The open circuit voltage (OCV) and the total resistance of stack R_{stack} (Ω) were calculated from graphical method by using the linear correlation between voltage and current:

$$V(I) = OCV - R_{stack}I \tag{6}$$

Similarly, maximum gross power density P_d (W/m^2) was calculated by using parabolic correlation between power density and current density i (A/m^2):

$$P_d(i) = ai^2 + bi \tag{7}$$

and maximum value obtained from following equation:

$$P_{d,\max} = -\frac{b^2}{4a} \tag{8}$$

3. Results and discussion

Our results are reported and discussed in four distinct sections. Initially, findings on the physical membrane properties of the novel sPES membranes are presented and compared with the commercial CMX and Fujifilm membranes. In the second part, the trend of membrane permselectivity for various ionic gradient is discussed, while in the third part membrane ionic resistance measurements are elaborated. Finally, in the fourth section, reverse electrodialysis power densities are measured for the newly developed membranes and compared with commercial reference membranes.

3.1. Physical membrane properties

Relevant properties of lab-made homogeneous cation exchange membranes and reference commercial membranes were characterized in order to estimate their potential for RED. Results are reported in Table 2. CMX, a commercial CEM manufactured by Astom Corp. Ltd., Japan, is one of the most investigated membrane under RED conditions due to its good permselectivity, ion conductivity and mechanical stability. The backbone of CMX is made of sulfonated polystyrene-divinylbenzene and it is reinforced by a polyvinyl chloride support [37].

The measured electro-physical properties of CMX showed a good agreement with previously reported data. Dlugolecki et al. (2008) detected IEC, water uptake and the thickness as 1.62 meq·g^{-1}, 18% and 164 μm [23]. Similarly, Safranova et al. (2016) studied CMX and reported 1.78 meq·g^{-1} IEC, 17% water uptake and 175 μm thickness [37].

Fuji-CEM-Type 1, which is reinforced by a hydrated polyolefin support, was characterized as a second benchmark cation exchange membrane. Again, a good agreement was observed with previously reported properties, 61% water uptake and 125 μm thickness while IEC was measured to be 14% higher [38].

sPES-P and sPES-D were prepared on a glass support by using sulfonated polyethersulfone without any reinforcement or crosslinking agent (the abbreviations P and D refer asymmetric membrane with non-connected pores and dense membrane, respectively). The measured values of IEC for sPES-P and sPES-D were similar (only a slight difference of 3.5% was observed) and comparable to the IEC value of 1.19 meq·g^{-1} provided by the manufacturer of sulfonated polyethersulfone. The final cross-section morphology of these membranes, prepared by solvent evaporation and immersion precipitation, are shown in Fig. 6a–c and Fig. 6b–d, respectively. As expected, the membrane prepared by the solvent evaporation exhibited a dense structure, without visible porosity at micrometric scale; this was supported by the transparency of sPES-D at a visual inspection. On the other hand, an open-structured membrane was formed when immersion precipitation method was used, with asymmetrically distributed pores with diameter lower than 1 μm and not interconnected. The white color of the film was also an indirect implication of this morphology. The final thicknesses of sPES-D and sPES-P membranes were significantly lower than commercial membranes. Since the membrane thickness is proportional to the resistance, thin membranes are beneficial to boost the RED performance in the circumstance that interfacial resistances and solution resistances are not dominant over membrane resistance. Although a recent study revealed that the effect of membrane thickness on RED performance is not significant for mimicked seawater/river water mixing [39], for more concentrated ionic streams it is certainly expected that thinner membranes will allow better performance.

Although sPES-D and sPES-P were made of the same polymer, noticeable difference on water uptake values were observed; in particular, the observed 2.4 fold increase for the sPES-P membrane is coherent with its morphology. In an ion exchange membrane, fixed ionic groups attract the water and form a hydration shell around them. For sPES-D exhibiting a dense structure, it is expected that all the water released during drying the membrane is associated to hydration shell. However, for sPES-P, entrapped water within pores and interstitial gaps also contributes to water uptake. Therefore, the interpretation of the electro-physical properties of sPES-P membrane, over the measured water uptake and charge density values in Table 2, can be misleading since the entrapped water cannot be immediately related to intrinsic electro-physical properties of the polymer.

Immersion precipitation or solvent evaporation are normally not the most preferred manufacturing methods for ion exchange membranes despite their wide acceptance in industrial practice. Since the fixed charged moieties of polymer matrix attract the water, having a self-standing polymer film becomes more difficult with increasing ion exchange capacity [28]; moreover, polymers can become water soluble at an extreme IEC. Therefore, a mechanically weak and gel-like structure is formed when the content of fixed charged groups is too high. In this study, to overcome this problem, a sulfonated polyethersulfone with a relatively low IEC (1.19 meq·g^{-1}) was selected, whereas the IEC of the commercial CEMs is usually significantly higher. For example, IEC of Selemion CMV and Fumasep FKE were measured as 2.01 and 1.36 meq·g^{-1}, respectively [23] while, in this study, Neosepta CMX and Fujifilm Type1 were 1.61 and 1.96 meq·g^{-1}. Although, the lower IEC of our membranes could lead to inferior performance, we are convinced that the significantly lower cost associated with easy manufacturing methods and the lack of a required support, still make these membrane highly attractive.

Table 2
Some membrane properties.

Membrane	Thickness[a] (μm)	IEC (meq·g^{-1})	Water uptake (%)[a]	Charge density[a] (mol/L)	Presence of support
sPES-P	83 ± 6	1.15 ± 0.02	67.2 ± 0.5	1.7 ± 0.06	No
sPES-D	63 ± 6	1.19 ± 0.04	28.0 ± 0.4	4.3 ± 0.57	No
CMX	166 ± 1	1.61 ± 0.03	25.5 ± 0.1	6.3 ± 0.23	Yes
FUJI-CEM	121 ± 1	1.96 ± 0.02	54.9 ± 1.4	3.6 ± 0.27	Yes

[a] Values are given at 0.5 M NaCl.

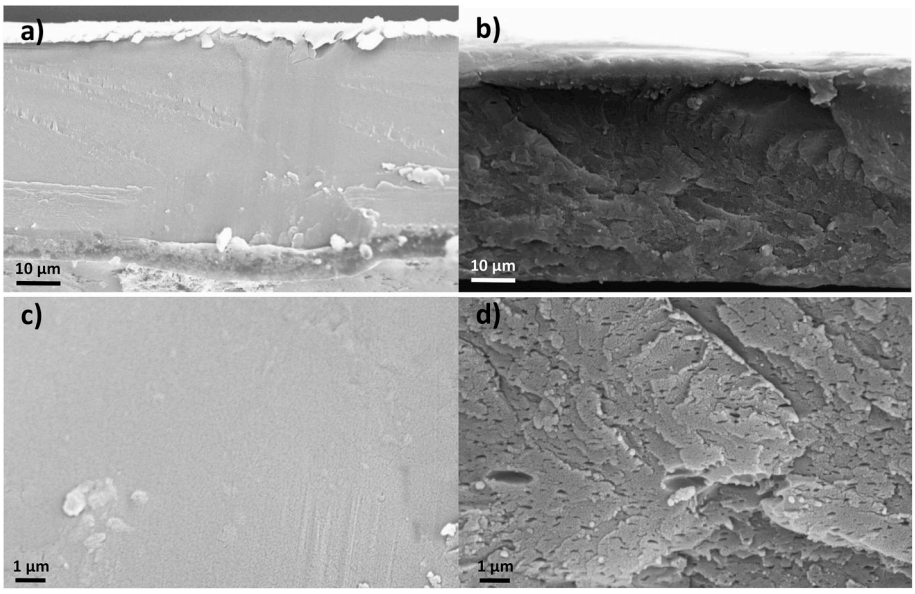

Fig. 6. Cross section of sPES-D membrane at; a) 3000x, c) 20000x; cross section of sPES-P membrane at b) 3000x, d) 20000x.

It is known that the concentrated salt solutions act as a non-solvent for polyelectrolytes [40], since the repulsive electrostatic interactions between fixed charge groups force the polymer to form a stretched configuration in a low ionic strength solution. Conversely, a high ion concentration of the coagulation bath shields the fixed charge groups electrostatic repulsion, so the polyelectrolyte segments reorganize itself from soluble to insoluble arrangement and it precipitates. Therefore, 5 M NaCl solution was used to induce phase separation: excess Na^+ ions shielded fixed SO_3^- groups of sPES and a white film was precipitated.

Besides electrochemical properties, mechanical stability of IEMs is also very important, considering that expected life time is 5–10 years under different feed concentrations, and especially when membranes are exposed to hypersaline brines. From a practical point of view, sPES membranes were able to withstand the conditions of RED experiment and all physical and electrochemical characterization carried out in this study, although the thickness of lab-made membranes was relatively low. Since commercial membranes were prepared with a support, their thickness is limited to the thickness of support; on the other hand, the thickness of lab-made membranes can be easily arranged by setting casting thickness.

For a feasible RED operation, the price of the ion exchange membranes is required to be less than 2 €/m^2 [27]. Immersion precipitation can be beneficial to reduce IEM price to this desired value by consuming less material during the membrane manufacturing step when it is compared to solvent evaporation. Casting thickness/final thickness ratio for sPES-D and sPES-P were 7.9 and 3.0, respectively; thus, approximately 2.6 times less material is required to prepare a membrane with the same thickness. In addition, low IEC of sPES (1.19 meq·g^{-1}) is expected to reduce cost in the sulfonation step.

3.2. Permselectivity

The membrane permselectivity indicates the ability to select counter ions over co-ions; most of the commercial ion exchange membranes have a permselectivity higher than 0.90. Previous studies showed, however, that the membrane permselectivity strongly depends on the concentration of the test solutions. Although the permselectivity can be close to the ideal value of 1.00 in diluted solutions, more realistic process solutions or brines can lower the permselectivity [41]. Therefore, CEMs were tested in different concentration gradients, i.e. 0.1/0.5, 0.1/4.0 and 0.5/4.0 M NaCl solution pairs.

Fig. 7 compares the permselectivity data of CMX, Fuji-CEM, sPES-P and sPES-D versus different NaCl gradients at 25 °C. In standard solution (0.1/0.5 M NaCl), the measured permselectivity for CMX was practically ideal (α = 1.00), while for Fuji-CEM and sPES-D it was a little lower at 0.95, and for sPES-P it was 0.84. The high charge density (6.3 mol/L) of CMX leads to excellent co-ion exclusion and allows only counter ions to pass, while the moderate charge density of sPES-D and Fuji-CEM causes some co-ion transport from the high to the low concentration compartment. On the other hand, low permselectivity of sPES-P can be attributed to its porous structure which causes inefficient Donnan exclusion due to presence of defects or occurrence of interstitial concentration polarization.

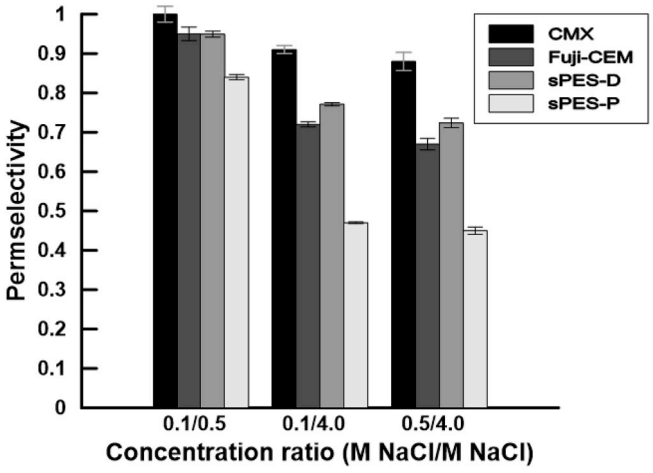

Fig. 7. Permselectivity of sPES-P, sPES-D, Fuji-CEM and CMX at different NaCl concentrations (temperature: 25 °C, flowrate: 460 ml/min).

Increasing the concentration gradient to 0.1/4.0 M NaCl caused a notable decrease in the permselectivity of all membranes. Loss in permselectivity by 9%, 19%, 24% and 44% was observed for CMX, sPES-D, Fuji-CEM and sPES-P, respectively. Similarly, increasing the low compartment concentration (0.5/4.0 M NaCl) further reduced the permselectivity of all CEMs.

A correlation exists between permselectivity, charge density and solution concentration. For a dilute, ideal and monovalent electrolyte solution, Donnan equilibrium can be simplified to following equation

[42]:

$$C_{co}^{m} = \frac{C_{co}^{2}}{C_{fix}^{m}} \quad (9)$$

where C^{m}_{co} is co-ion concentration in the membrane phase, C_{co} is co-ion concentration in the solution interface and C^{m}_{fix} is the fixed charged group concentration of the membrane. Consequently, an efficient Donnan exclusion can be obtained at low feed concentration and high charge density because the co-ion concentration of the membrane is expected to be low. Accordingly, the decreasing permselectivity with increasing feed concentration as well as increasing permselectivity with increasing charge density can be explained by expected effect related to Donnan exclusion theory.

3.3. Electrochemical impedance spectroscopy

Electrochemical impedance spectroscopy is a powerful characterization method to quantify and distinguish membrane and solution resistance (R_{m+s}), diffusion boundary layer (R_{dbl}) and electrical double layer resistances (R_{edl}) at different alternating current frequencies. The membrane and solution resistance can be represented as a resistor (Fig. 5) and its response is obtained at high frequency. The fixed groups on the membrane surface attract oppositely charged ions from the solution and form the electrical double layer which can be represented as a parallel resistor and a capacitor: the response can be observed in the Nyquist plot with a semi-circle at medium frequency. The diffusion boundary layer is related to different ion transport numbers in the membrane and the bulk phase; just as the electrical double layer, the diffusion boundary layer gives a semi-circle pattern in the Nyquist plot at low frequency. It can be represented as a pair of a resistor and a constant phase element in the equivalent circuit [43].

Fig. 8 illustrates CMX, Fuji-CEM, sPES-P and sPES-D responses to AC current in 0.01–1000 Hz range in Nyquist plot with 0.5 M NaCl solution recirculated at 460 ml/min and 25 °C. R_{m+s} values were measured at 1000 Hz where the curve intersects Z' axis, which represents the real part of the impedance. At this condition, R_{m+s} order for CEMs were: CMX > Fuji-CEM > sPES-D > sPES-P. Similarly, the total non-ohmic resistance can be compared roughly by investigating the magnitude of the curves in the Z" axis which is the imaginary part of the impedance. Non-ohmic resistance of sPES-P was significantly less than the other CEMs while dense CEMs resulted in comparable values.

The Nyquist plots of sPES-P at different NaCl concentration are shown in Fig. 9 after substracting R_{m+s}. As can be seen from the 0.1 M NaCl data the Nyquist curve has two overlapping semi-cycle: the one at higher frequency belongs to the electrical double layer and its resistance was less significant. On the other hand, the diffusion boundary layer was prevalent especially at low concentration. Increasing the solution concentration from 0.1 to 2.0 M NaCl reduces the magnitude of R_{edl} and R_{dbl}, and non-ohmic resistance contribution became insignificant

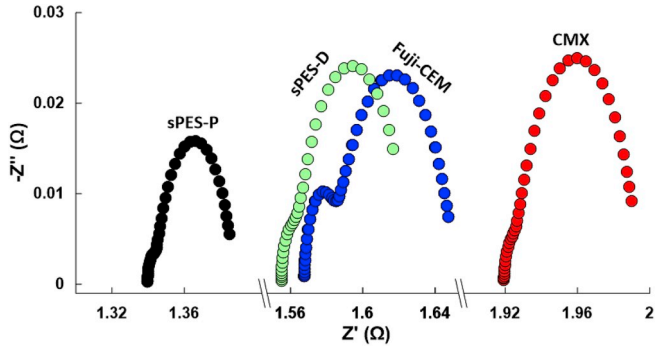

Fig. 8. Nyquist plot of CMX, Fuji-CEM, sPES-P and sPES-D at 0.5 M NaCl solution (temperature: 25 °C, flowrate: 460 ml/min).

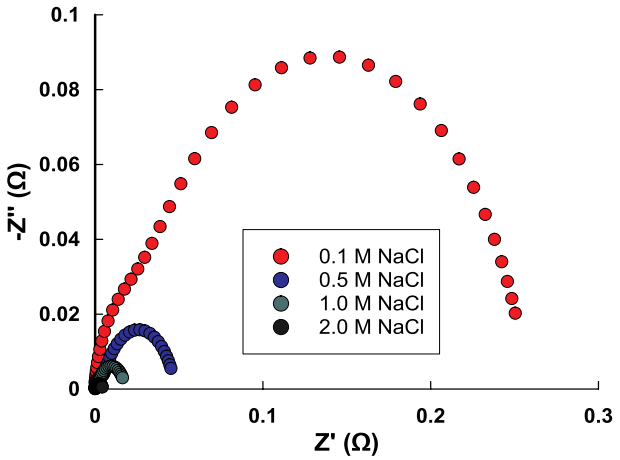

Fig. 9. Nyquist plot of sPES-P for 0.1, 0.5, 1.0 and 2.0 M NaCl solution at 25 °C and 460 ml/min (membrane + solution resistance R_{m+s} is substracted).

compared to the membrane resistance. The electrochemical characterization of CMX by Dlugolecki et al. (2010) revealed that R_{dbl} was dominant over R_m in 0.017 M NaCl, while in 0.5 M NaCl, the dominant resistance became R_m. However, it is also stated that R_{dbl} can be decreased 3–4 times by increasing the flow rate from 100 to 800 ml/min, while R_m and R_{edl} were independent of flow rate [20].

The bar chart in Fig. 10 summarizes the resistance analysis results after fitting the impedance spectroscopy data to the equivalent circuit (Fig. 5). Among the investigated CEMs, and for all concentrations, the highest and the lowest membrane resistance were obtained for CMX and sPES-P, respectively, whilst Fuji-CEM and sPES-D resulted in moderate and comparable membrane resistance. For Fuji-CEM and sPES-D, R_m did not show a clear trend and remained stable between 1.00 and 1.20 $\Omega \cdot cm^2$ range with varying concentration. On the other hand, CMX resistance increased from 1.69 to 2.64 $\Omega \cdot cm^2$ and sPES-P resistance decreased from 0.48 to 0.22 $\Omega \cdot cm^2$ when the concentration was increased from 0.1 to 4.0 M NaCl.

Membrane properties such as thickness, water uptake and charge density are associated to ionic resistance [39,44]. Having low thickness and an open structure with non-connected pores, sPES-P exhibited the lowest ionic resistance. When sPES-D and CMX membrane resistance is compared, even though CMX had a higher charge density, sPES-D resulted in a lower resistance due to higher water uptake and significantly lower thickness. On the other side, when comparing Fuji-CEM and sPES-D, it can be concluded that high water uptake of Fuji-CEM compensates the decrease on resistance due to its high thickness and low charge density. Therefore, both CEMs had comparable ionic resistance.

It is possible to conclude a tradeoff relationship between the permselectivity and the resistance. Geise et al. (2013) studied the electrochemical properties and structure property relationship of anion exchange membranes and attributed the resistance-permselectivity tradeoff to the water volume fraction of the membranes. Membranes absorbing more water resulted in low permselectivity and low ionic resistance and vice versa [44]. Similarly, in this study, the resistance and the permselectivity increased with decreasing water uptake value (see Table 2).

Fig. 10 indicates that, at low concentration (i.e. 0.1 M NaCl), non-ohmic resistances can be as dominant as ohmic resistance: 64%, 47%, 46% and 42% of total resistance were contributed by non-ohmic resistances for sPES-P, sPES-D, Fuji-CEM and CMX, respectively. Even though the highest percentage was obtained for sPES-P, the lowest non-ohmic resistance was measured for sPES-P at all concentrations. The contribution of the electrical double layer to the overall non-ohmic resistance ranged from 6% to 9%, and for a solution concentration

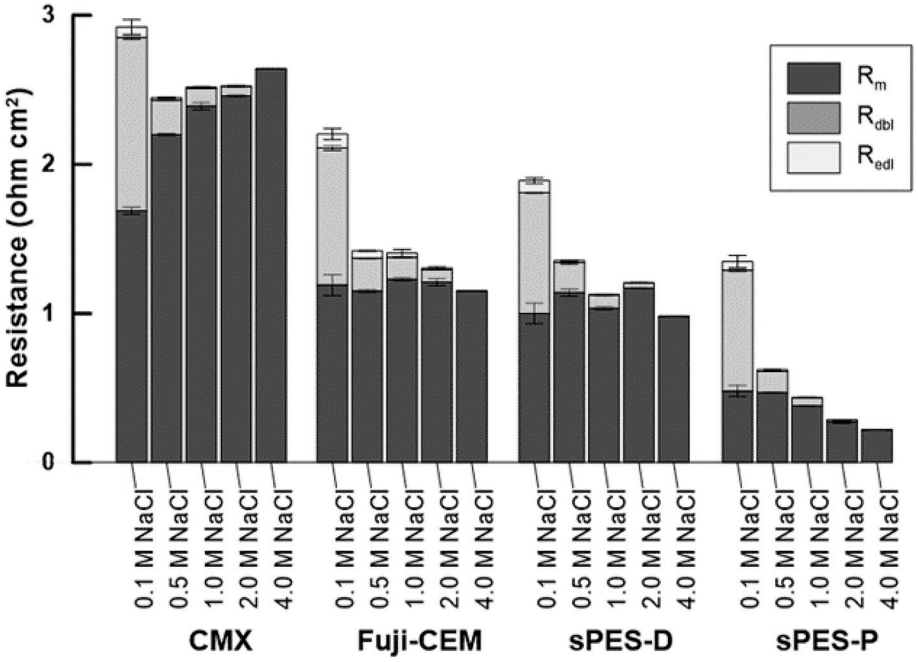

Fig. 10. Comparison of R_m, R_{edl} and R_{dbl} of CEMs at different concentrations.

greater than 1.0 M NaCl, it reduced to less than 1%. R_{dbl} diminished progressively until becoming insignificant at high concentrations: 0.01, 0.03, 0.06 and 0.08 Ω·cm^2 of R_{dbl} were measured for sPES-P, sPES-D, CMX and Fuji-CEM in 2 M NaCl, respectively. These results were in accordance with other studies reported in literature. Fontananova et al. (2017) characterized Fuji-CEM 80050 at varying NaCl concentration. At 0.1 M NaCl, more than 50% of the total resistance was contributed by non-ohmic resistance at 275 ml/min and 25 °C; however, it reduced to 5% approximately, when 4.0 M NaCl was recirculated as test solution [45]. In a study by Galama et al. (2014), non-ohmic resistance of CMX was found to contribute by 51% and 11% to the total resistance in 0.1 and 1.1 M NaCl solutions, respectively, with flow rate of 170 ml/min and temperature of 25 °C [46].

3.4. Reverse electrodialysis performance

Fig. 11 illustrates the polarization curves of RED stack installed with CMX, Fuji-CEM-Type1, sPES-D and sPES-P for 0.1/4.0 M NaCl solution at 25 °C.

The open circuit voltages were measured as 0.314 V, 0.305 V, 0.298 V and 0.291 V for sPES-D, CMX, Fuji-CEM-Type1 and sPES-P, respectively. Although, permselectivity of CMX was superior (see Fig. 7), surprisingly, OCV of CMX was found lower than sPES-D. This discrepancy could be attributed to high diffusion boundary layer resistance of CMX; $R_{dbl,CMX}$ and $R_{dbl,\ sPES\text{-}D}$ in 0.1 M NaCl were 1.16 and 0.81 Ω, respectively (see Fig. 10). So, due to higher $R_{dbl,CMX}$, concentration gradient across the membrane and therefore OCV is lowered.

The stack resistances (R_{stack}) varied from 0.229 Ω to 0.194 Ω with a decreasing order of CMX > sPES-D > Fuji-CEM-Type1 > sPES-P. Stacks equipped with CMX and sPES-P were in accordance with the aforementioned electrochemical impedance results (see section 3.3). On the other hand, R_{stack} of s-PES-D was 10% higher than R_{stack} of Fuji-CEM-Type while impedance results indicated their resistance were comparable for 0.1 M and 4 M NaCl. It is worth noting that solutions at the same concentration were circulated on both surface of the membrane during impedance experiments while membranes were exposed to 0.1/4/0 M NaCl concentration gradient under RED conditions. It is therefore likely that the membrane resistance can vary under RED operation. For example, Galama et al. (2014) investigated the resistance of CMX in 0.1/1.1 M NaCl were 3.87 Ω cm^2, whereas it was 5.74 Ω cm^2 and 3.04 Ω cm^2 in 0.1/0.1 M NaCl and 1.1/1.1 M NaCl, respectively [46].

Fig. 12 compares the gross power density (P_d) of CMX, Fuji-CEM-Type1, sPES-D and sPES-P for 0.1/4.0 M NaCl. The highest measured P_d was 3.92 W/$m^2_{m,MP}$ for sPES-D while the lowest was 3.23 W/$m^2_{m,MP}$ for

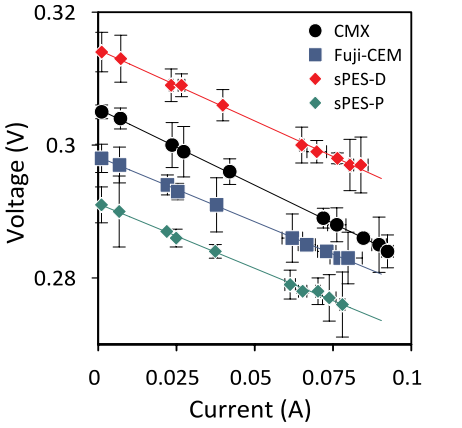

Fig. 11. Voltage vs. current for 0.1/4.0 M NaCl at 25 °C.

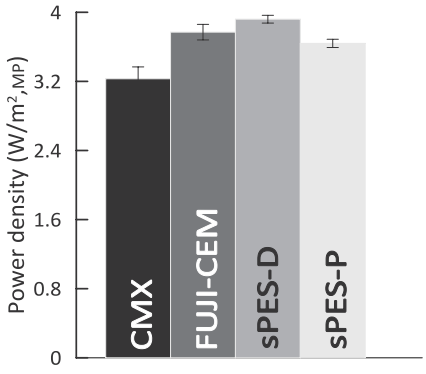

Fig. 12. Power density of CEMs for 0.1/4.0 M NaCl at 25 °C.

CMX. In addition, utilizing Fuji-CEM-Type1 and sPES-P resulted in 17% and 13% higher power density than CMX. Although, CMX and sPES-P were superior CEMs regarding permselectivity and resistance, respectively, they are outperformed by Fuji-CEM-Type1 and sPES-D. Therefore, P_d results indicates that an optimization of permselectivity and resistance is essential for the RED IEMs design.

4. Conclusions and outlook

In this study, a sulfonated polyethersulfone (sPES) polymer with 1.19 $meq \cdot g^{-1}$ IEC was used to prepare membranes by solvent evaporation or immersion precipitation phase inversion methods, obtaining dense (sPES-D) or asymmetric membranes with non-connected pores (sPES-P), respectively. To our knowledge, for the first time sPES lab-made CEMs were prepared and characterized for their RED potential, with specific focus on operations at high salinity gradients in order to exploit the potential of hyper-concentrated brines. Beside lab-made membranes, commercial Neosepta CMX and Fujifilm CEM Type 1 were characterized at the same conditions as reference.

RED gross power densities pointed out that sPES membranes can represent an interesting alternative to the present commercial membranes. Interestingly, with respect to benchmark membranes, higher power density was obtained for lab-made sPES membranes with brackish water (0.1 M NaCl)/hypersaline brine (4 M NaCl) feeds. In the light of these results, it can be concluded that there is a real opportunity to further optimize sPES based membranes for RED.

Besides the preparation of novel RED membranes, the membrane materials and techniques used in this study might have the potential to overcome the economic barriers that work against RED commercialization. Presently, the price of the IEMs is considered as one of the most challenging limitation in the renewable energy market. In this work, sPES membranes were manufactured from polyethersulfone, a relatively cheap hydrocarbon polymer, using very simple and easily scalable production approaches. Therefore, a cheap production line could be created that would require less raw material (thinner membranes) and no supports, with strong potential to decrease the CEM price to the targeted threshold of 2 €/m^2. Moreover, power generation in RED is the product of the potential difference and the current density. The potential difference and the current density are proportional to membrane permselectivity and conductivity, respectively. Therefore, ion exchange membrane optimization based on permselectivity/resistance tradeoff is expected to reduce the cost of produced power for a unit membrane area.

Declaration of competing interest

The authors declare that they have no known competing financial interests or personal relationships that could have appeared to influence the work reported in this paper.

Acknowledgements

The financial support of:

- the Education, Audiovisual and Culture Executive Agency (EACEA-EU) within the programme EUDIME “Erasmus Mundus Doctorate in Membrane Engineering” (FPA 2011–0014, SGA 2014–0970, http://eudime.unical.it);

- the Ministry of Education, University and Research (MIUR) of Italy within the project ERANETMED3-166 EXTRASEA “Extracting water, minerals and energy from seawater desalination brine”

is kindly acknowledged. The authors also thank Dr. Jeff Wood for his helpful discussions. In addition, the authors would like to thank Konishi Chemical Ind. Co. Ltd. for providing sulfonated polyethersulfone polymer, Neosepta for CMX and Fujifilm Manufacturing for Fuji-CEM-Type 1.

References

[1] R.E. Pattle, Production of electric power by mixing fresh and salt water in the hydroelectric pile, Nature 174 (1954) 660.
[2] O.A. Alvarez-Silva, A.F. Osorio, C. Winter, Practical global salinity gradient energy potential, Renew. Sustain. Energy Rev. 60 (2016) 1387–1395.
[3] A.H. Avci, R.A. Tufa, E. Fontananova, G. Di Profio, E. Curcio, Reverse Electrodialysis for energy production from natural river water and seawater, Energy 165 (2018) 512–521.
[4] E. Farrell, M.I. Hassan, R.A. Tufa, A. Tuomiranta, A.H. Avci, A. Politano, E. Curcio, H.A. Arafat, Reverse electrodialysis powered greenhouse concept for water- and energy-self-sufficient agriculture, Appl. Energy 187 (2017) 390–409.
[5] M. Tedesco, E. Brauns, A. Cipollina, G. Micale, P. Modica, G. Russo, J. Helsen, Reverse Electrodialysis with saline waters and concentrated brines: a laboratory investigation towards technology scale-up, J. Membr. Sci. 492 (2015) 9–20.
[6] R.E. Lacey, Energy by reverse electrodialysis, Ocean Eng. 7 (1980) 1–47.
[7] W. Li, W.B. Krantz, E.R. Cornelissen, J.W. Post, A.R.D. Verliefde, C.Y. Tang, A novel hybrid process of reverse electrodialysis and reverse osmosis for low energy seawater desalination and brine management, Appl. Energy 104 (2013) 592–602.
[8] E. Brauns, Towards a worldwide sustainable and simultaneous large-scale production of renewable energy and potable water through salinity gradient power by combining reversed electrodialysis and solar power? Desalination 219 (2008) 312–323.
[9] A.H. Avci, P. Sarkar, R.A. Tufa, D. Messana, P. Argurio, E. Fontananova, G. Di Profio, E. Curcio, Effect of Mg2+ ions on energy generation by Reverse Electrodialysis, J. Membr. Sci. 520 (2016) 499–506.
[10] R.A. Tufa, E. Rugiero, D. Chanda, J. Hnàt, W. van Baak, J. Veerman, E. Fontananova, G. Di Profio, E. Drioli, K. Bouzek, E. Curcio, Salinity gradient power-reverse electrodialysis and alkaline polymer electrolyte water electrolysis for hydrogen production, J. Membr. Sci. 514 (2016) 155–164.
[11] R.A. Tufa, E. Curcio, W. Van Baak, J. Veerman, S. Grasman, E. Fontananova, G. Di Profio, Potential of brackish water and brine for energy generation by salinity gradient power-reverse electrodialysis (SGP-RE), RSC Adv. 4 (2014) 42617–42623.
[12] J.W. Post, H.V.M. Hamelers, C.J.N. Buisman, Energy recovery from controlled mixing salt and fresh water with a reverse electrodialysis system, Environ. Sci. Technol. 42 (2008) 5785–5790.
[13] C. Klaysom, T.Y. Cath, T. Depuydt, I.F.J. Vankelecom, Forward and pressure retarded osmosis: potential solutions for global challenges in energy and water supply, Chem. Soc. Rev. 42 (2013) 6959–6989.
[14] S. Chou, R. Wang, L. Shi, Q. She, C. Tang, A.G. Fane, Thin-film composite hollow fiber membranes for pressure retarded osmosis (PRO) process with high power density, J. Membr. Sci. 389 (2012) 25–33.
[15] N.Y. Yip, M. Elimelech, Comparison of energy efficiency and power density in pressure retarded osmosis and reverse electrodialysis, Environ. Sci. Technol. 48 (2014) 11002–11012.
[16] J.W. Post, J. Veerman, H.V.M. Hamelers, G.J.W. Euverink, S.J. Metz, K. Nymeijer, C.J.N. Buisman, Salinity-gradient power: evaluation of pressure-retarded osmosis and reverse electrodialysis, J. Membr. Sci. 288 (2007) 218–230.
[17] D.A. Vermaas, D. Kunteng, M. Saakes, K. Nijmeijer, Fouling in reverse electrodialysis under natural conditions, Water Res. 47 (2013) 1289–1298.
[18] R.K. Nagarale, G.S. Gohil, V.K. Shahi, Recent developments on ion-exchange membranes and electro-membrane processes, Adv. Colloid Interface Sci. 119 (2006) 97–130.
[19] J. Veerman, R.M. de Jong, M. Saakes, S.J. Metz, G.J. Harmsen, Reverse electrodialysis: comparison of six commercial membrane pairs on the thermodynamic efficiency and power density, J. Membr. Sci. 343 (2009) 7–15.
[20] P. Długołęcki, B. Anet, S.J. Metz, K. Nijmeijer, M. Wessling, Transport limitations in ion exchange membranes at low salt concentrations, J. Membr. Sci. 346 (2010) 163–171.
[21] R. Ghalloussi, L. Chaabane, C. Larchet, L. Dammak, D. Grande, Structural and physicochemical investigation of ageing of ion-exchange membranes in electrodialysis for food industry, Separ. Purif. Technol. 123 (2014) 229–234.
[22] E. Guler, Y. Zhang, M. Saakes, K. Nijmeijer, Tailor-made anion-exchange membranes for salinity gradient power generation using reverse electrodialysis, ChemSusChem 5 (2012) 2262–2270.
[23] P. Dlugolecki, K. Nymeijer, S. Metz, M. Wessling, Current status of ion exchange membranes for power generation from salinity gradients, J. Membr. Sci. 319 (2008) 214–222.
[24] J.G. Hong, B. Zhang, S. Glabman, N. Uzal, X. Dou, H. Zhang, X. Wei, Y. Chen, Potential ion exchange membranes and system performance in reverse electrodialysis for power generation: a review, J. Membr. Sci. 486 (2015) 71–88.
[25] R.A. Tufa, S. Pawlowski, J. Veerman, K. Bouzek, E. Fontananova, G. di Profio, S. Velizarov, J. Goulão Crespo, K. Nijmeijer, E. Curcio, Progress and prospects in reverse electrodialysis for salinity gradient energy conversion and storage, Appl. Energy 225 (2018) 290–331.
[26] E. Güler, R. Elizen, D.A. Vermaas, M. Saakes, K. Nijmeijer, Performance-determining membrane properties in reverse electrodialysis, J. Membr. Sci. 446 (2013) 266–276.
[27] J.W. Post, C.H. Goeting, J. Valk, S. Goinga, J. Veerman, H.V.M. Hamelers, P.J.F. M. Hack, Towards implementation of reverse electrodialysis for power generation from salinity gradients, Desalin. Water Treat. 16 (2010) 182–193.
[28] H. Strathmann, Ion-Exchange Membrane Separation Processes, Elsevier B.V, Amsterdam, The Netherlands, 2004.
[29] M. Turek, B. Bandura, Renewable energy by reverse electrodialysis, Desalination 205 (2007) 67–74.

[30] A. Daniilidis, R. Herber, D.a. Vermaas, Upscale potential and financial feasibility of a reverse electrodialysis power plant, Appl. Energy 119 (2014) 257–265.
[31] J.G. Hong, Y. Chen, Nanocomposite reverse electrodialysis (RED) ion-exchange membranes for salinity gradient power generation, J. Membr. Sci. 460 (2014) 139–147.
[32] H.-K. Kim, M.-S. Lee, S.-Y. Lee, Y.-W. Choi, N.-J. Jeong, C.-S. Kim, High power density of reverse electrodialysis with pore-filling ion exchange membranes and a high-open-area spacer, J. Mater. Chem. A. 3 (2015) 16302–16306.
[33] T. Sata, Ion Exchange Membranes: Preparation, Characterization, Modification and Application, The Royal Society of Chemistry, Cambridge, UK, 2004.
[34] A.K. Hołda, I.F.J. Vankelecom, Understanding and Guiding the Phase Inversion Process for Synthesis of Solvent Resistant Nanofiltration Membranes, 2015, pp. 1–17, 42130.
[35] E. Fontananova, W. Zhang, I. Nicotera, C. Simari, W. van Baak, G. Di Profio, E. Curcio, E. Drioli, Probing membrane and interface properties in concentrated electrolyte solutions, J. Membr. Sci. 459 (2014) 177–189.
[36] W.M. Haynes, CRC Handbook of Chemistry and Physics, 96th ed., CRC Press/Taylor and Francis, Boca Raton, FL, 2016.
[37] E.Y. Safronova, D.V. Golubenko, N.V. Shevlyakova, M.G. D'yakova, V.A. Tverskoi, L. Dammak, D. Grande, A.B. Yaroslavtsev, New cation-exchange membranes based on cross-linked sulfonated polystyrene and polyethylene for power generation systems, J. Membr. Sci. 515 (2016) 196–203.
[38] T. Rijnaarts, E. Huerta, W. Van Baak, K. Nijmeijer, Effect of divalent cations on RED performance and cation exchange membrane selection to enhance power densities, Environ. Sci. Technol. 51 (2017) 13028–13035.
[39] M. Tedesco, H.V.M. Hamelers, P.M. Biesheuvel, Nernst-Planck transport theory for (reverse) electrodialysis: III. Optimal membrane thickness for enhanced process performance, J. Membr. Sci. 565 (2018) 480–487.
[40] V.A. Izumrudov, M.Y. Gorshkova, I.F. Volkova, Controlled phase separations in solutions of soluble polyelectrolyte complex of DIVEMA (copolymer of divinyl ether and maleic anhydride), Eur. Polym. J. 41 (2005) 1251–1259.
[41] A. Zlotorowicz, R.V. Strand, O.S. Burheim, S. Kjelstrup, The permselectivity and water transference number of ion exchange membranes in reverse electrodialysis, J. Membr. Sci. 523 (2017) 402–408.
[42] M. Mulder, Basic Principles of Membrane Technology, Kluwer Academic Publishers, The Netherlands, 1996.
[43] J.-S. Park, J.-H. Choi, J.-J. Woo, S.-H. Moon, An electrical impedance spectroscopic (EIS) study on transport characteristics of ion-exchange membrane systems, J. Colloid Interface Sci. 300 (2006) 655–662.
[44] M. Geise, M.A. Hickner, B.E. Logan, Ionic resistance and permselectivity tradeoffs in anion exchange membranes, Appl. Mater. Interfaces 5 (2013) 10294–10301.
[45] E. Fontananova, D. Messana, R.A. Tufa, I. Nicotera, V. Kosma, E. Curcio, W. Van Baak, E. Drioli, G. Di Profio, Effect of solution concentration and composition on the electrochemical properties of ion exchange membranes for energy conversion, J. Power Sources 340 (2017) 282–293.
[46] A.H. Galama, D.A. Vermaas, J. Veerman, M. Saakes, H.H.M. Rijnaarts, J.W. Post, K. Nijmeijer, Membrane resistance: the effect of salinity gradients over a cation exchange membrane, J. Membr. Sci. 467 (2014) 279–291.